Polyanthraquinone-Based Organic Cathode for High-Performance Rechargeable Magnesium-Ion Batteries

*Baofei Pan, Jinhua Huang, Zhenxing Feng, Li Zeng, Meinan He, Lu Zhang, John T. Vaughey, Michael J. Bedzyk, Paul Fenter, Zhengcheng Zhang, Anthony K. Burrell, and Chen Liao**

With regard to the growing environmental crisis resulted from the rapid worldwide energy consumption, energy harvested from sustainable and renewable sources like solar, wind, or tide is desirable. However, the lack of efficient and economical energy storage devices is still the bottleneck for the practical application of these clean energies. Albeit the great success of lithium-ion batteries (LIBs) in the field of portable electronic applications, the cost and safety barriers make the state-of-the-art LIBs not suitable for large power storage or transmission. As alternative solutions, multivalent-ion batteries, such as Mg, Ca, or Al, are promising as the new generation energy storage devices due to their advantages in safety, cost, and capacity.[1] Therefore, many efforts have been devoted to the development of high-performance multivalent-ion batteries in recent years.[1,2] Inspired by the pioneer work by Aurbach et al. in 2000 with the design of the prototype Mg-Mo_6S_8 battery,[3] the interest in advanced secondary magnesium-ion batteries blossomed. In recent years, in contrast to the rapid progress of effective electrolytes capable of plating/stripping magnesium reversibly with wide electrochemical windows,[4] the development of efficient cathode material is far behind. Materials such as MnO_2,[5] V_2O_5,[6] and even novel layered oxyfluoride[7] have been reported to facilitate Mg^{2+} ion intercalation; however, they also have problems such as irreversible intercalation and low capacity. The incompatibility of the state-of-the-art magnesium electrolytes with metal oxide cathode materials is still problematic to afford high energy density magnesium batteries. New approach to design metal oxide compatible electrolyte has received more attention recently, such as the ionic liquid-base magnesium electrolytes with efficient magnesium plating/stripping performance.[8] However, to date, Chevrel phase Mo_6S_8 is still the most reliable cathode material with long-term cycling performance in rechargeable magnesium-ion batteries. However, Mo_6S_8 only has a theoretical capacity of around 130 mAh g^{-1}, and could only operate at less than 1.3 V (vs Mg), which is not desirable for high density energy storage. Thus, the pursuit of higher voltage and higher capacity cathode material deserves great attention for magnesium-ion batteries nowadays. Redox-active organic material is another type of promising alternative for magnesium-ion batteries, especially in terms of the resource sustainability and environmental friendliness. To our surprise, although the great success has been achieved for organic cathodes in lithium- and sodium-ion batteries,[9] only a handful of organic cathodes have been reported for magnesium-ion batteries in the literature.[10] A common issue for the organic cathodes is that either they could only deliver low capacity even at very slow current rates, or they suffer from considerable capacity loss upon cycling. To implement a stable and sustainable magnesium-ion battery system, herein, we report the development of two new anthraquinone-base polymers, 2,6-polyanthraquinone (26PAQ) and 1,4-polyanthraquinone (14PAQ), as high-performance cathode materials for rechargeable magnesium-ion batteries. 1,5-poly(anthraquinonylsulfide) (PAQS) was also tested as a baseline material for the magnesium-ion batteries, among the three polyanthraquinone materials we evaluated, namely, PAQS, 26PAQ, and 14PAQ. 14PAQ shows the best electrochemical performance for rechargeable magnesium-ion batteries. The nomenclature of anthraquinone[11] and the structures of PAQS, 26PAQ, and 14 PAQ were shown in **Scheme 1** for clarification.

The redox-active anthraquinonyl moieties have already rendered PAQS as very effective Li^+ or Na^+ storage reservoir.[9c,12] Recently, Dominko and co-workers also reported the performance of the Mg-PAQS batteries using several non-nucleophilic magnesium electrolytes, such as MACC ($MgCl_2$-$AlCl_3$), MHCC ($Mg(HMDS)_2$-$AlCl_3$), and MTCC ($Mg(TFSI)_2$-$MgCl_2$).[10e] We also validated the same PAQS polymer as cathode material for magnesium-ion batteries using our own non-nucleophilic electrolyte.[13] The presence of carbonyl groups in the anthraquinonyl moieties prevents the use of any nucleophilic magnesium electrolytes, such as the well-known Grignard-based APC ($PhMgCl$-$AlCl_3$) or DCC (nBu_2Mg + $EtAlCl_2$) electrolytes.[3,14] Thus, the non-nucleophilic 0.3 M $Mg(HMDS)_2$-$4MgCl_2$ (HMDS: hexamethyldisilazide) in THF (tetrahydrofuran) solution was chosen as the electrolyte in this study.[13] The quite similar capacity decay phenomenon has also been observed in our Mg-PAQS batteries when $Mg(HMDS)_2$-$4MgCl_2$/THF was used as the electrolyte. As shown in **Figure 1**, although the good Coulombic efficiency can be observed in the cyclic voltammetry

Dr. B. Pan, Dr. J. Huang, Dr. Z. Feng, M. He, Dr. L. Zhang, Dr. J. T. Vaughey, Dr. P. Fenter, Dr. Z. Zhang, Dr. A. K. Burrell, Dr. C. Liao
Joint Center for Energy Storage Research
Chemical Science and Engineering Division
Argonne National Laboratory
Lemont, IL 60439, USA
E-mail: liaoc@anl.gov

L. Zeng, Prof. M. J. Bedzyk
Applied Physics Program
Department of Materials Science and Engineering and Department of Physics and Astronomy
Northwestern University
Evanston, IL 60208, USA

DOI: 10.1002/aenm.201600140

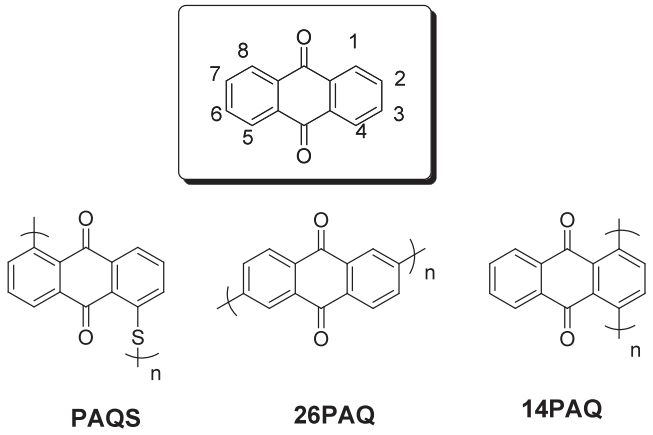

Scheme 1. The nomenclature of anthraquinone and the chemical structures of PAQS, 26PAQ, and 14PAQ.

measurement, the capacity continues to decay, and eventually only around 30 mAh g^{-1} discharge capacity was retained after 100th cycle (70% capacity loss). The Coulombic efficiency is calculated as high as 94% for the first cycle, and dropped to 88% for the second cycle; however, it came back to above 99% after cycle 11 and stays very high (> 99%) through the rest of the 100 cycles.

The high capacity decay indicates that PAQS is not capable of providing sustainable and long-term cycling performance. However, the excellent chemical reversibility still suggests that the redox-active organic cathode is a very promising material for the development of high-performance magnesium-ion batteries, especially if the capacity retention could be further improved. One of the merits of organic electrodes is the structure flexibility, which allows for the feasible functionalization to suppress the electrode dissolution. The major issue with the PAQS system arises from the dissolution of the anthraquinone polymer, and therefore we designed different polymers in order to improve the battery performance. Coincidentally, a recent account reporting the polyanthraquinone system for lithium-ion batteries was recently published while we are summarizing our quinonyl polymer structure variation studies for the magnesium batteries, and the strategies were developed in order to solve the same problem.[15]

Two anthraquinone-based polymers, 26PAQ and 14PAQ, aiming at improving the capacity retention for advanced magnesium-ion batteries, were synthesized according to the modified literature procedures (see the Supporting Information for details).[16] As shown in **Figure 2**, both the two polymers have shown excellent chemical reversibility in the cyclic voltammogram (CV) measurements using the 0.3 M $Mg(HMDS)_2$-4$MgCl_2$/THF electrolyte. For 26PAQ, two reduction phases were observed at around 1.71 and 1.52 V(vs Mg/Mg^{2+} and the same reference was used hereafter), respectively, corresponding to the stepwise two-electron reduction processes from neutral 26PAQ to $[26PAQ]^{2-}$ anions. While only one broad subsequent oxidation phase was detected in CV at about 2.0 V, making the two redox couplings of 26PAQ at about 1.85 and 1.75 V. Similarly, two reduction peaks were also observed for 14PAQ at 1.57 and 1.48 V, and the two subsequent oxidations took place at 1.67 and 1.79 V, respectively. Thus, the stepwise two-electron redox potentials of 14PAQ were experimentally measured at about 1.6 and 1.7 V, which are slightly lower than that of 26PAQ.

Having established the excellent chemical reversibility of 26PAQ and 14PAQ in the 0.3 M $Mg(HMDS)_2$-4$MgCl_2$/THF electrolyte, their cycling performance was then investigated in magnesium-ion batteries. As shown in **Figure 3**a,c, at a moderate current rate of 0.5 C (130 mA g^{-1}), 26PAQ cell can initially deliver 122 mAh g^{-1} discharge capacity, which is slightly better than the performance of PAQS. To our satisfaction, no serious capacity loss was observed in the following cycles. Albeit the capacity decay is still present, the discharge capacity remained at 100.2 mAh g^{-1} after 100th cycle (82% capacity retention), which is drastically improved compared to the behavior of the PAQS system (30% capacity retention). In contrast to this slow but continuing capacity loss of 26PAQ battery cell, 14PAQ presents a much better cycling stability. As shown in Figure 3b,d, at the same current rate of 0.5 C (130 mA g^{-1}), the considerable

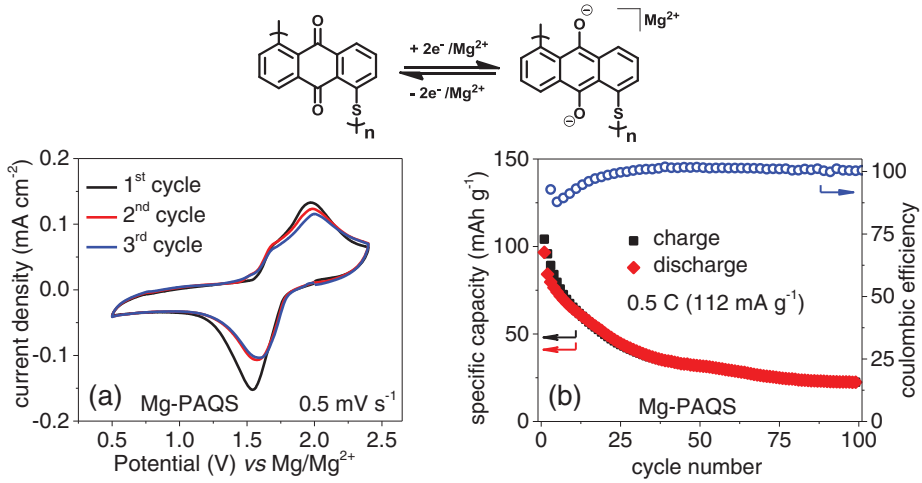

Figure 1. Electrochemical and cycling performance of Mg-PAQS cells using 0.3 M $Mg(HMDS)_2$-4$MgCl_2$/THF as the electrolyte: a) steady-state cyclic voltammetry of Mg-PAQS cell at a scan rate of 0.5 mV s^{-1}; b) capacities and Coulombic efficiency at a current rate of 0.5 C (112 mA g^{-1}).

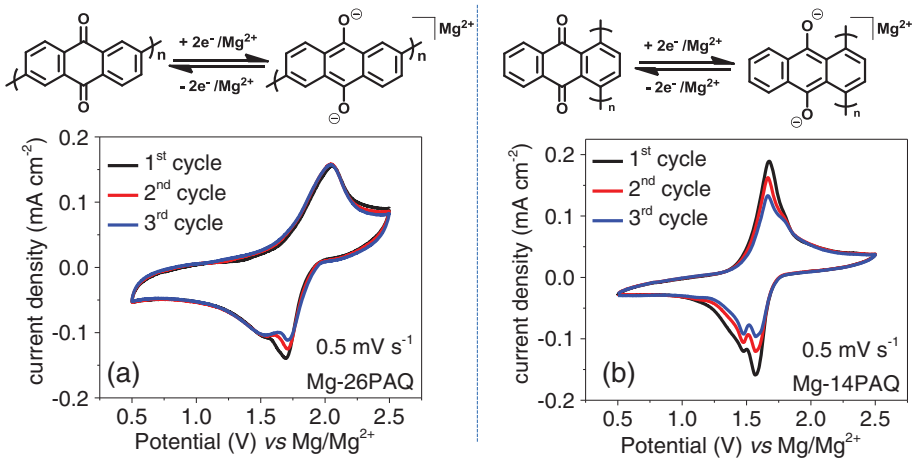

Figure 2. Typical steady-state cyclic voltammetry using 0.3 M $Mg(HMDS)_2$-$4MgCl_2$/THF as the electrolyte (0.5 mV s^{-1}): a) Mg-26PAQ cell; b) Mg-14PAQ cell.

capacity loss was only observed in the first seven cycles from 132.7 to 106.0 mAh g^{-1}, and since then very little capacity loss was detected in at least 100 cycles. A discharge capacity of 104.9 mAh g^{-1} can be obtained in the 100th cycle, which only suggests a 1% capacity loss since the 7th cycle. In addition to good capacity retention, Mg-14PAQ battery cell also showed higher Coulombic efficiency (>99% in the 100th cycle) than that of Mg-26PAQ cell (97.4% in the 100th cycle). In contrast to PAQS or 26PAQ, besides being superior in capacity retention, the Mg-14PAQ also shows a much smaller discharge–charge polarization, and no significant electrochemical polarization increase was observed in at least 100 cycles. A similar small polarization was also observed for 14PAQ in Li-ion batteries, which was attributed to the much smaller HOMO–LUMO (highest occupied molecular orbital-lowest unoccupied molecular orbital*) gap in the molecular level compared to other polyanthraquinonyl derivatives.[15] In addition to the excellent cycling performance at a 0.5 C rate, the rate performance of 14PAQ was then evaluated by the stepwise cycling experiment from 0.5 C (130 mAh g^{-1}) to 5.0 C (1300 mAh g^{-1}) (20 cycles for

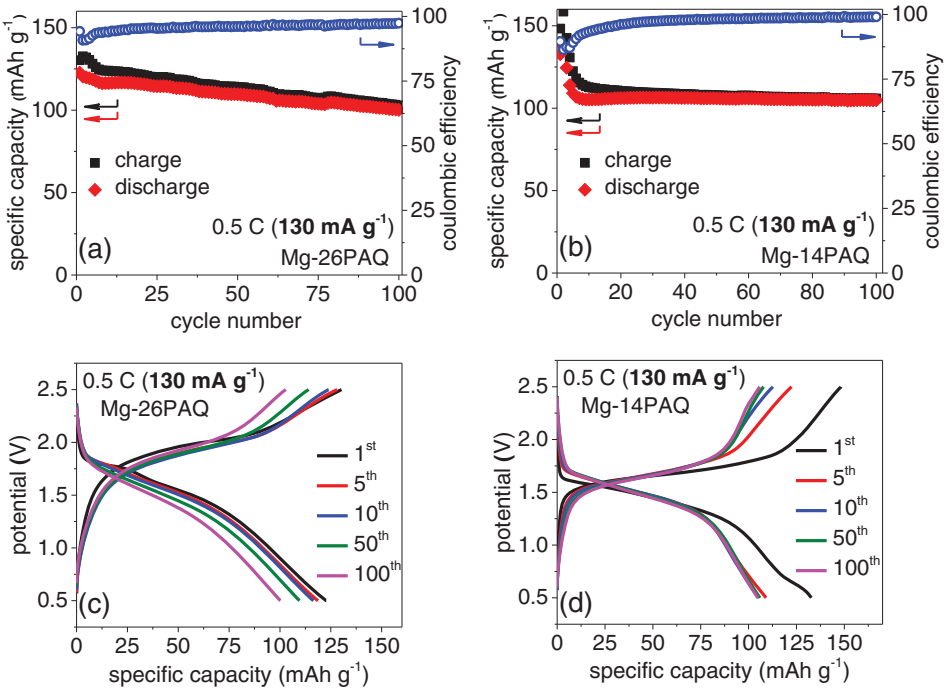

Figure 3. a) Mg-26PAQ: capacities and Coulombic efficiency profiles at a current rate of 0.5 C (130 mA g^{-1}); b) Mg-14PAQ: capacities and Coulombic efficiency profiles at a current rate of 0.5 C (130 mA g^{-1}); c) Mg-26PAQ, representative discharge–charge galvanostatic curves; d) Mg-14PAQ, representative discharge–charge galvanostatic curves.

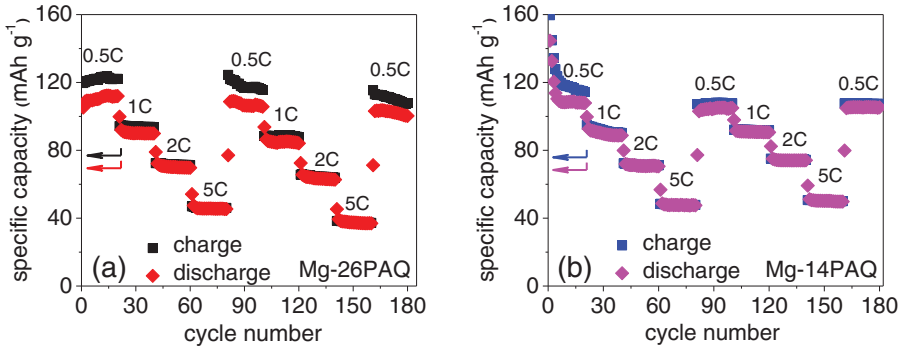

Figure 4. Stepwise rate capacity with increasing current rates: a) Mg-26PAQ cell at the current rates of 0.5, 1.0, 2.0, and 5.0 C; b) Mg-14PAQ cell at the current rates of 0.5, 1.0, 2.0, and 5.0 C.

each current rate). As shown in **Figure 4**b, the demonstrated cycling stability further highlights the great potential 14PAQ as high-rate and long-term cycling cathode material for rechargeable magnesium-ion batteries. In agreement with the rate capacity performance, as shown in **Figure 5** at the elevated current rates of 1 C (260 mA g^{-1}) and 2 C (520 mA g^{-1}), the Mg-14PAQ cells were further proved to be capable of delivering more than 1000 cycles with very small amount of capacity loss and high Coulombic efficiency. For instance, at a current rate of 1 C (260 mA g^{-1}), a similar capacity decay was detected only in the first 10 cycles from 110.1 to 87.1 mAh g^{-1}. After the 10th cycle, very little amount of capacity loss was observed, and the discharge capacities of 83.7 and 78.7 mAh g^{-1} can be recovered in the 500th and 1000th cycles (Coulombic efficiency > 99.7%) , which suggests a capacity retention of 96.1% and 90.4%, respectively. At faster current rates such as 2 C and 5 C, slightly decreased capacities were obtained. The sustainable cycling performance of Mg-14PAQ battery was further highlighted by the excellent galvanostatic discharge–charge behavior after more than 600 h continuing cycling, as shown in Figure 5b.

Electrode dissolution was believed to be the major issue accounting for the considerable capacity fading when using organic polymers as electrodes in rechargeable batteries. However, the dissolution of the polymers in their neutral state only represents half of the story, as the solubility and stability of the reduced state (upon discharging) are equally important. Since all the three polymers, PAQS, 26PAQ, and 14PAQ, have shown very limited solubility in the electrolyte solvent THF, the stability and solubility in their reduced states could be responsible for the difference in the cycling performance. As shown in Figure S12 (Supporting Information), upon discharging for each battery cell, the glass fiber separator from Mg-PAQS cell shows intense orange color, indicating the significant electrode dissolution during the discharging process. In contrast, very little color change has been detected in 26PAQ and 14PAQ. The results suggest that the electrode dissolution is more serious for PAQS, which results in the poor cycling performance and rapid capacity loss upon cycling. Since both 26PAQ and 14PAQ have very limited solubility both in their neutral and reduced states in THF, the structure difference likely accounts for the difference in the long-term cycling performance. Unlike the structurally rigid polymer chain of 26PAQ, the redox-active quinonyl moieties in 14PAQ lie on the side of the main polymer chain, which allows the rotation flexibility of the anthraquinonyl groups along the polymer chain. This rotation flexibility helps minimize the space hindrance and relax the structural stress of the polymer, which in turn provides better structure stability for 14PAQ in comparison with 26PAQ. In addition, upon the discharging, the inserted magnesium cation species can be better stabilized by the two adjacent carbonyl (C=O) groups via the chelating effect. A similar chelating coordination bonding model has also been demonstrated to account for the enhanced cycling performance when a redox-active quinone-based organic polymer was used in Li-ion batteries.[17] In addition to the overall improved long-term cycling performance of 14PAQ, the rapid capacity loss in the first few cycles also deserves attention. We speculate that the two adjacent carbonyl groups (C=O) could only stably accommodate one inserted magnesium cation species due to the induced steric hindrance resulted from the chelating interaction. Thus, the stabilized capacity of 14PAQ is only half of its theoretical capacity, and this is in agreement with the experimental observation.

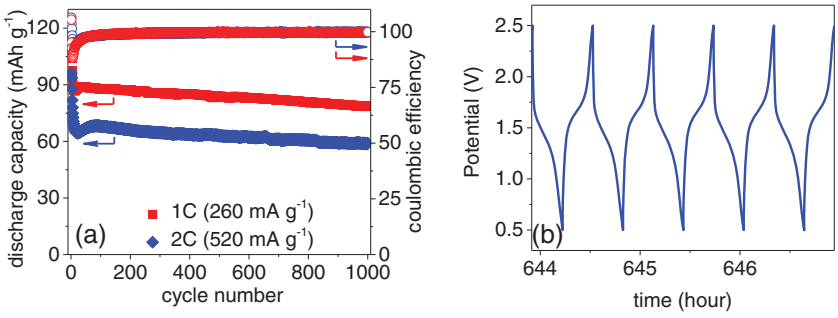

Figure 5. Mg-14PAQ cycling performance: a) 1000 cycles discharge capacity and Coulombic efficiency for current rates at 1 C (260 mA g^{-1}) and 2 C (520 mA g^{-1}); b) galvanostatic discharge–charge curves from 996th to 1000th cycles for a current rate of 1 C (260 mA g^{-1}).

In order to gain in-depth redox understanding behind the excellent cycling performance of our Mg-14PAQ battery system, X-ray photoelectron spectroscopy (XPS)

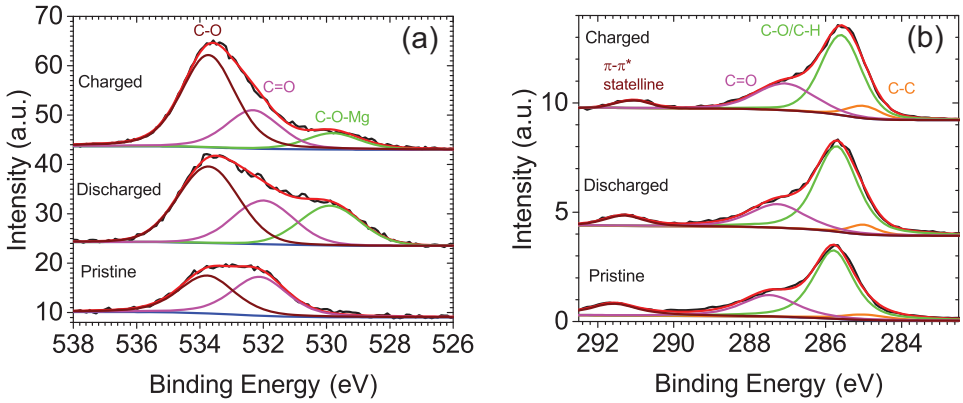

Figure 6. X-ray photoelectron spectra: a) O_{1s}; b) C_{1s}.

measurements were carried out to investigate the bonding and composition changes for the organic cathodes. **Figure 6**a shows the O_{1s} spectra comparison for the pristine, discharged, and charged states. Clearly, the pristine cathode has negligible C–O–metal (Mg) component (529.9 eV),[18] while the discharged cathode shows significant C–O–Mg component, suggesting the interaction of magnesium ions with the C=O bond and the formation of the C–O–Mg structure. The subsequent charging process suppressed the C–O–Mg signal in the O_{1s} spectrum, indicating the recovery of the oxidized 14PAQ from the reduced state. This formation of C–O–Mg is a result as the C=O bond breaks and forms C–O–Mg during discharge, and the decrease of the C–O–Mg peak indicates that upon charge, the C–O–Mg returns to C=O bond. The high-resolution C_{1s} spectra in Figure 6b also support the conclusion that the C=O transformed to C–O–Mg during discharge. Since the carbon is the majority of 14PAQ laminate and the binding energy of C–O (285.5–286.5 eV) is overlapped with C–H in 14PAQ,[19] the changes of C=O and C–O peaks in Figure 6b are not easy to see due to overall strong carbon signal, but the quantitative ratio changes can be determined from XPS analysis (Table S1, Supporting Information). Therefore, the redox mechanism involving the reversible C=O to C–O–Mg transformation (i.e., upon the discharging the anthraquinone moieties undergo the reduction to generate hydroxyanthraquinone anions, along with the transformation of C=O double bonds to C–O single bonds) can be established from our XPS measurement, which is similar to the proposed redox mechanism for a few reported quinone-based Li or Na-organic battery systems.[9c,12]

In summary, a series of anthraquinonyl-based polymers have been prepared and evaluated as high-performance organic cathode for rechargeable Mg-ion batteries. Excellent chemical reversibility can be obtained for all the three candidates, PAQS, 26PAQ, and 14PAQ. However, the inherent capacity decay suggests that PAQS is not capable of providing sustainable cycling performance in magnesium-ion batteries. Whereas, the replacement of PAQS by 26PAQ successfully suppressed the capacity fading, and the Mg-26PAQ battery cell can deliver above 100 mAh g^{-1} discharge capacity in 100 cycles (82% capacity retention) at a reasonable rate of 0.5 C (130 mA g^{-1}). In contrast to this slow but still continuing capacity fading of the Mg-26PAQ batteries, the Mg-14PAQ system shows the best cycling stability among the series. The considerable capacity loss was only observed in the first few cycles for Mg-14PAQ battery cells, and very small amount of capacity loss was observed in the next hundreds of cycles. For instance, at a current rate of 0.5 C (130 mA g^{-1}), 104.9 mAh g^{-1} discharge capacity can be obtained in the 100th cycle, which suggests a 99% capacity retention since the 7th cycle. This superior cycling stability and rate capacity of the Mg-14PAQ system were further highlighted by more than 1000 successful cycles at elevated current rates with small amount of capacity loss. In addition to be superior to other reported organic cathodes for rechargeable magnesium-ion batteries, our Mg-14PAQ system also represents one of the very few magnesium-ion battery systems capable of providing stable and long-term cycling performance. While compared to the state-of-the-art Chevrel Mo_6S_8 (below 1.3 V discharge voltage), Mg-14PAQ can be operated at much higher working voltages (about 1.6 V discharge voltage at a current rate of 0.5 C), and capable of delivering much higher capacities both theoretically and experimentally. The success of the Mg-14PAQ system further highlights the potential of magnesium-ion battery as the new generation energy storage devices, and will also benefit for the continuing development of low cost and environmentally benign redox-active organic cathode materials with higher energy density for the magnesium storage.

Experimental Section

General Consideration: All synthesis and characterization were carried out in argon-filled glove boxes or argon-filled Schlenk line unless otherwise noted. Chemicals were purchased commercially and used without further purification. $Mg(HMDS)_2$-$4MgCl_2$/THF electrolyte, PAQS, 26PAQ, and 14PAQ were all prepared according to reported procedures (see the Supporting Information for details).

Cathode Laminate Preparation: The laminates were prepared by mixing the active organic polymer material, Timcal Super C45 carbon black, and poly(vinylidene difluoride) binder with a weight ratio of 4:5:1 by *N*-methyl-2-pyrrolidione, and the resulting slurry was coated onto Graftech Grafoil graphite foil. The laminates were dried in a 75 °C oven for 2 h before they were cut into electrodes with a diameter of 7/16 in. The electrode laminates were then dried in vacuum at 120 °C for more than 12 h before use. Each laminate contained around 1.0–1.5 mg of active material.

Electrochemical Measurement: CV measurement was carried out using a Princeton Instrument's Parstat MC potentiostat, and three consecutive

cycles were performed for each experiment. CV of the electrolyte was carried out using three-electrode setup with platinum disc (2 mm in diameter, CH instruments, Austin, TX) as the working electrode and freshly polished magnesium ribbons (Sigma-Aldrich, > 99.5% Mg basis) as the counter and reference electrodes. CV of the cathode material was carried out with the two-electrode setup in the 2032-type coin cells using cathode laminate as a working electrode, freshly polished magnesium disc (7/16 in.) as both the counter and reference electrodes, and the 0.3 M $Mg(HMDS)_2$-$4MgCl_2$/THF as the electrolyte. The cell cycling performance was carried out using the 2032-type coin cells on a Maccor series 4000 cycler with the cutoff of 0.5 and 2.5 V at room temperature.

X-Ray Photoelectrospectroscopy: The XPS spectra were collected at the Keck II facility of NUANCE at Northwestern University with an Omicron ESCA probe using monochromated Al Kα X-rays. A low-energy electron flood gun was used to compensate the XPS-induced surface charging effects. The carbon 1s line (284.8 eV) was used as the reference to calibrate the XPS spectra.

Supporting Information

Supporting Information is available from the Wiley Online Library or from the author.

Acknowledgements

This work was supported as part of the Joint Center for Energy Storage Research, an Energy Innovation Hub funded by the U.S. Department of Energy, Office of Science, Basic Energy Sciences. The submitted manuscript was created by UChicago Argonne, LLC, Operator of Argonne National Laboratory (Argonne). Argonne, a U.S. Department of Energy Office of Science laboratory, is operated under Contract No. DE-AC02-06CH11357. This work made use of Northwestern University Central Facilities supported by the Materials Research Science and Engineering Center (MRSEC) through National Science Foundation (NSF) under Contract No. DMR-1121262.

Received: January 22, 2016
Revised: March 29, 2016
Published online: May 9, 2016

[1] a) H. D. Yoo, I. Shterenberg, Y. Gofer, G. Gershinsky, N. Pour, D. Aurbach, *Energy Environ. Sci.* **2013**, *6*, 2265; b) P. Saha, M. K. Datta, O. I. Velikokhatnyi, A. Manivannan, D. Alman, P. N. Kumta, *Prog. Mater. Sci.* **2014**, *66*, 1; c) J. Muldoon, C. B. Bucur, T. Gregory, *Chem. Rev.* **2014**, *114*, 11683.

[2] a) M.-C. Lin, M. Gong, B. Lu, Y. Wu, D.-Y. Wang, M. Guan, M. Angell, C. Chen, J. Yang, B.-J. Hwang, H. Dai, *Nature* **2015**, *520*, 324; b) Z. Feng, X. Chen, L. Qiao, A. L. Lipson, T. T. Fister, L. Zeng, C. Kim, T. Yi, N. Sa, D. L. Proffit, A. K. Burrell, J. Cabana, B. J. Ingram, M. D. Biegalski, M. J. Bedzyk, P. Fenter, *ACS Appl. Mater. Interfaces* **2015**, *7*, 28438.

[3] D. Aurbach, Z. Lu, A. Schechter, Y. Gofer, H. Gizbar, R. Turgeman, Y. Cohen, M. Moshkovich, E. Levi, *Nature* **2000**, *407*, 724.

[4] a) Z. Zhao-Karger, X. Y. Zhao, O. Fuhr, M. Fichtner, *RSC Adv.* **2013**, *3*, 16330; b) O. Tutusaus, R. Mohtadi, T. S. Arthur, F. Mizuno, E. G. Nelson, Y. V. Sevryugina, *Angew. Chem. Int. Ed. Engl.* **2015**, *54*, 7900; c) J. Muldoon, C. B. Bucur, A. G. Oliver, T. Sugimoto, M. Matsui, H. S. Kim, G. D. Allred, J. Zajicek, Y. Kotani, *Energy Environ. Sci.* **2012**, *5*, 5941; d) T. Liu, Y. Shao, G. Li, M. Gu, J. Hu, S. Xu, Z. Nie, X. Chen, C. Wang, J. Liu, *J. Mater. Chem. A* **2014**, *2*, 3430; e) Y.-S. Guo, F. Zhang, J. Yang, F.-F. Wang, Y. NuLi, S.-I. Hirano, *Energy Environ. Sci.* **2012**, *5*, 9100; f) R. E. Doe, R. Han, J. Hwang, A. J. Gmitter, I. Shterenberg, H. D. Yoo, N. Pour, D. Aurbach, *Chem. Commun.* **2014**, *50*, 243; g) T. J. Carter, R. Mohtadi, T. S. Arthur, F. Mizuno, R. G. Zhang, S. Shirai, J. W. Kampf, *Abstr. Pap. Am. Chem. Soc.* **2014**, *248*; h) T. J. Carter, R. Mohtadi, T. S. Arthur, F. Mizuno, R. G. Zhang, S. Shirai, J. W. Kampf, *Angew. Chem. Int. Ed.* **2014**, *53*, 3173.

[5] J.-S. Kim, W.-S. Chang, R.-H. Kim, D.-Y. Kim, D.-W. Han, K.-H. Lee, S.-S. Lee, S.-G. Doo, *J. Power Sources* **2015**, *273*, 210.

[6] S. Tepavcevic, Y. Liu, D. Zhou, B. Lai, J. Maser, X. Zuo, H. Chan, P. Král, C. S. Johnson, V. Stamenkovic, N. M. Markovic, T. Rajh, *ACS Nano* **2015**, *9*, 8194.

[7] J. T. Incorvati, L. F. Wan, B. Key, D. Zhou, C. Liao, L. Fuoco, M. Holland, H. Wang, D. Prendergast, K. R. Poeppelmeier, J. T. Vaughey, *Chem. Mater.* **2016**, *28*, 17.

[8] a) F. Bertasi, C. Hettige, F. Sepehr, X. Bogle, G. Pagot, K. Vezzù, E. Negro, S. J. Paddison, S. G. Greenbaum, M. Vittadello, V. Di Noto, *ChemSusChem* **2015**, *8*, 3069; b) T. Watkins, A. Kumar, D. A. Buttry, *J. Am. Chem. Soc.* **2016**, *138*, 641; c) M. Kar, Z. Ma, L. M. Azofra, K. Chen, M. Forsyth, D. R. MacFarlane, *Chem. Commun.* **2016**, *52*, 4033.

[9] a) Y. L. Liang, Z. L. Tao, J. Chen, *Adv. Energy Mater.* **2012**, *2*, 742; b) B. Haupler, A. Wild, U. S. Schubert, *Adv. Energy Mater.* **2015**, *5, 1402034*; c) Z. Song, H. Zhan, Y. Zhou, *Chem. Commun.* **2009**, 448.

[10] a) H. Senoh, H. Sakaebe, H. Sano, M. Yao, K. Kuratani, N. Takeichi, T. Kiyobayashi, *J. Electrochem. Soc.* **2014**, *161*, A1315; b) H. Sano, H. Senoh, M. Yao, H. Sakaebe, T. Kiyobayashi, *Chem. Lett.* **2012**, *41*, 1594; c) Y. Nuli, Z. P. Guo, H. K. Liu, J. Yang, *Electrochem. Commun.* **2007**, *9*, 1913; d) S. Y. Ha, Y. W. Lee, S. W. Woo, B. Koo, J. S. Kim, J. Cho, K. T. Lee, N. S. Choi, *ACS Appl. Mater. Interfaces* **2014**, *6*, 4063; e) J. Bitenc, K. Pirnat, T. Bančič, M. Gaberšček, B. Genorio, A. Randon-Vitanova, R. Dominko, *ChemSusChem* **2015**, *8*, 4128; f) M. M. Huie, D. C. Bock, E. S. Takeuchi, A. C. Marschilok, K. J. Takeuchi, *Coord. Chem. Rev.* **2015**, *287*, 15.

[11] G. P. Moss, *Pure Appl. Chem.* **1998**, *70*, 143.

[12] W. Deng, X. Liang, X. Wu, J. Qian, Y. Cao, X. Ai, J. Feng, H. Yang, *Sci. Rep.* **2013**, *3*, 2671.

[13] C. Liao, N. Sa, B. Key, A. K. Burrell, L. Cheng, L. A. Curtiss, J. T. Vaughey, J. J. Woo, L. B. Hu, B. F. Pan, Z. C. Zhang, *J. Mater. Chem. A* **2015**, *3*, 6082.

[14] O. Mizrahi, N. Amir, E. Pollak, O. Chusid, V. Marks, H. Gottlieb, L. Larush, E. Zinigrad, D. Aurbach, *J. Electrochem. Soc.* **2008**, *155*, A103.

[15] Z. Song, Y. Qian, M. L. Gordin, D. Tang, T. Xu, M. Otani, H. Zhan, H. Zhou, D. Wang, *Angew. Chem. Int. Ed.* **2015**, *54*, 13947.

[16] a) Y. Zhou, B. Wang, C. Liu, N. Han, X. Xu, F. Zhao, J. Fan, Y. Li, *Nano Energy* **2015**, *15*, 654; b) Z. Song, Y. Qian, M. L. Gordin, D. Tang, T. Xu, M. Otani, H. Zhan, H. Zhou, D. Wang, *Angew. Chem.* **2015**, *127*, 14153.

[17] Z. Song, Y. Qian, X. Liu, T. Zhang, Y. Zhu, H. Yu, M. Otani, H. Zhou, *Energy Environ. Sci.* **2014**, *7*, 4077.

[18] H.-C. Lee, Y.-C. Huang, T.-F. Liu, W.-T. Whang, C.-G. Chao, *J. Adhes. Sci. Technol.* **2015**, *29*, 1229.

[19] H. Bouayad, Z. Wang, N. Dupré, R. Dedryvère, D. Foix, S. Franger, J. F. Martin, L. Boutafa, S. Patoux, D. Gonbeau, D. Guyomard, *J. Phys. Chem. C* **2014**, *118*, 4634.